

**Contract No:**

This document was prepared in conjunction with work accomplished under Contract No. DE-AC09-08SR22470 with the U.S. Department of Energy (DOE) Office of Environmental Management (EM).

**Disclaimer:**

This work was prepared under an agreement with and funded by the U.S. Government. Neither the U. S. Government or its employees, nor any of its contractors, subcontractors or their employees, makes any express or implied:

- 1 ) warranty or assumes any legal liability for the accuracy, completeness, or for the use or results of such use of any information, product, or process disclosed; or
- 2 ) representation that such use or results of such use would not infringe privately owned rights; or
- 3) endorsement or recommendation of any specifically identified commercial product, process, or service.

Any views and opinions of authors expressed in this work do not necessarily state or reflect those of the United States Government, or its contractors, or subcontractors.

## ADDITIVE MANUFACTURING FOR HYDROGEN APPLICATIONS

**M.J. MORGAN**

Savannah River National Laboratory  
Aiken SC, USA

**PAUL KORINKO**

Savannah River National Laboratory  
Aiken SC, USA

**WES EVERHART**

Kansas City National Security  
Campus, Kansas City, MO, USA

**JOHN BOBBITT**

Savannah River National Laboratory  
Aiken SC, USA

### **ABSTRACT**

Laser-based powder bed additive manufacturing was used to fabricate mechanical test specimens using Type 304L stainless steel using identical processing parameters. Three-point bend specimens were built vertically using a common scan strategy at plate locations with different surrounding heat sink conditions. Fracture toughness properties of as-built and hydrogen-precharged specimens were measured as a function of build location. The purpose was to develop an understanding of the effects of additive manufacturing (AM) build parameters and table conditions on fracture toughness and hydrogen compatibility. The results show that the fracture toughness properties of the as-built steels fell into two ranges: higher toughness and lower toughness. As-built toughness was lower than forged toughness. Fracture toughness values appeared to depend on the configuration of the heat sinks surrounding the specimen being built but no clear trend emerged from the data. Hydrogen precharging lowered the fracture toughness properties and changed the fracture mode.

### **INTRODUCTION**

Fracture toughness is a critical parameter for understanding the performance of additive manufacturing (AM) materials. Several publications have investigated the fracture toughness of a variety of materials from several AM processes [1-4]. Most previously completed studies investigated the effects of various heat treatments, and build directionalities.

Stainless steels have been an attractive choice for AM applications due to their high weldability and variety of valuable properties such as traditionally high toughness and ductility. Several studies have been completed specifically on Type 304L stainless steel and have investigated everything from parameter set development, tensile properties, microstructural evolution, and even the development of gradient materials within AM processes [5-8].

Several AM publications refer specifically to potential applications in exposure to hydrogen. Scotti, G. et al. [9] completed work with 316L stainless steel with respect to AM fuel cell components.

The purpose of this study was to begin to develop an understanding of the effects of AM build parameters and table conditions on fracture toughness and hydrogen compatibility of Type 304L austenitic stainless steel.

## EXPERIMENTAL PROCEDURE

For this research, a Renishaw AM250 SLM system was used. The AM250 uses a 1070 nm fiber laser with a maximum output of 200 watts (W) and an approximate spot diameter of 70  $\mu\text{m}$ . The composition of the Type 304L stainless steel powder is listed in Table 1. The powder used was 15-45  $\mu\text{m}$  in diameter. The Renishaw AM250 uses a point exposure scan pattern where a single point is exposed, the laser is turned off, repositioned, and then the next point is exposed. For each point the laser power is 200 W, the distance between points is 85  $\mu\text{m}$ , and the exposure time is 53  $\mu\text{sec}$ . The next layer is then scanned in the same way, however the pattern is rotated a specified amount. In addition to the hatch fill pattern, two border scans are used to smooth the outer profile. Previously developed 304L parameters sets were used for building samples on the AM250 [10]. In this way, a common scan strategy (Fig. 1) was used to fabricate mechanical test specimens with identical processing parameters.

Three different build geometries were completed in order to accommodate the various sample types and each build geometry was repeated three times to ensure a statistically significant number of samples. For all build geometries a given sample type was built within one quadrant of the build volume allowing for four sample types per build (Fig. 2). Each quadrant was again divided and organized in order to have three groups of vertical samples spanning the radial distance from the center of build plate with 10 mm, 20 mm, and 40 mm spacing between the centers of the samples in each group. This methodology was used to create build geometries encompassing unfinished tensile, unfinished high cycle fatigue, finished high cycle fatigue, unfinished low cycle fatigue, finished low cycle fatigue, impact, and torsion samples. In this paper, only the tensile and fracture toughness properties are considered.

Tensile samples were included within each build geometry to enable additional comparison of the different builds. Vertical samples were chosen as an indication of minimum properties based on the previous work discussed above and a diameter of 4.0 mm was chosen to provide a representative size of product that would be economical to produce using additive manufacturing. This size range is expected to provide a realistic probability for defects in the applied processes though ductility results may be skewed. Tensile properties of the AM samples were determined per ASTM E8 [12] at ambient temperature. Crosshead test speeds were controlled uniformly to minimize any impact of rate sensitivity and loading rates were approximately 620  $\text{MPa min}^{-1}$ .

Three-point bend specimens (Fig. 3) were built vertically using the common scan strategy described above. After fabrication, the specimens were notched and fatigue precracked. Some of the specimens were precharged with hydrogen for two weeks at 623 K and an over-pressure of 17 MPa and then stored in air in a freezer at 223 K until tested. The hydrogen content was estimated, using Ref

[12], to be  $\sim 2700$  appm. Fracture toughness properties of as-built and hydrogen-precharged specimens were measured as a function of build location. The properties were compared to the properties of forged Type 304L stainless steels having a similar composition (Table I).

The elastic-plastic J-integral was evaluated for all specimens at ambient temperature by loading to failure at  $0.002 \text{ mm-s}^{-1}$  while monitoring load, load-line displacement and crack extension (using a direct current potential-drop technique) using ASTM E1820-99 [13]. The samples used in the study were designed to be as thick as possible to maintain fracture surfaces with little or no necking and thin enough so that they could be saturated with hydrogen at a temperature that would not change the material microstructure during charging. For all test conditions, the requirements for thickness were not satisfied; therefore, all fracture toughness values are reported as unqualified  $J_Q$  values. While all fracture surfaces showed uniform crack fronts, only hydrogen-precharged specimens showed no evidence of shear lips along the sides of the specimens (implying plane-strain conditions prevailed for these specimens).

## RESULTS AND DISCUSSION

The as-built AM steel had a yield strength of 454 MPa, an ultimate strength of 626 MPa, and an elongation of 36%. These strength values are comparable to forged steels but the elongation values are lower (Table 2). Figure 4 show the typical load-displacement behavior for the AM steels that was observed during the three-point bend tests. For some of the as-built specimens, the load displacement curve exhibited a broad maximum prior to failure indicating high-toughness behavior. Other as-built specimens tended to show an immediate load drop at maximum load prior to failure indicating low toughness. Hydrogen precharged specimens showed a sharp load drop at maximum load at lower displacement values than as-built specimens.

Figure 5 shows the fracture toughness vs. crack extension (J-R) behavior for a number of the specimens tested. In general, the J-R curves for the as-built specimens fell into two toughness ranges – high or low toughness. The high-toughness specimens exhibited steep J-R curves while the low-toughness specimens were flattened. Overall the average fracture toughness value,  $J_Q$ , for the as-built AM steels was  $799 \pm 238 \text{ kJ/m}^2$ . Specimens in the high toughness group had an average toughness value of  $989 \pm 94 \text{ kJ/m}^2$  (5 specimens) and specimens in the low toughness group had an average toughness of  $560 \pm 58 \text{ kJ/m}^2$  (4 specimens).

Figures 4 and 5 show that hydrogen precharging lowered the resistance of the Type 304L as-built steels to cracking. The hydrogen precharged specimens had lower  $J_Q$  values (Table 2) and flatter J-R curves (Fig 5). A comparison with the fracture toughness values of forged steels is shown in Fig. 6. Forged steels had higher fracture toughness values and greater resistance to hydrogen-assisted cracking. The fracture appearance was consistent with the fracture toughness measurements. The fracture surfaces of the high-toughness AM steels had deeper more deformed dimples surrounding nonmetallic inclusions indicating a large amount of strain occurred prior to microvoid coalescence (Fig 7a). The

low toughness AM steels were flatter in appearance (Fig. 7b). The fracture appearance of hydrogen precharged specimens indicated quasi-cleavage and numerous secondary cracks (Fig 7c). The individual fracture toughness values as a function of build location identifiers are shown Table 3. At this time, no clear trend has emerged from the data, although it appears that specimens 3B1, 3A3, 3C1, and 3A9 which were built in relative isolation had higher fracture toughness values than those built with nearby heat sinks (3B4, 3B2, 3A1, and 3A5). More work is needed before a general conclusion can be drawn.

## CONCLUSIONS

The fracture toughness properties of as-built Type 304L stainless steel fell into two broad ranges – high toughness and low toughness.

The toughness differences may have been brought about by the configuration of the surrounding heat sinks during the AM build process. However, additional work is needed to clarify the scattering of the fracture toughness values as a function of build location.

Hydrogen reduced the fracture toughness value by 50-80% of the as-built toughness.

As-built AM steels had lower fracture toughness value and were less resistant to hydrogen-assisted cracking compared to forged steels.

## ACKNOWLEDGMENTS

Savannah River National Laboratory is operated by Savannah River Nuclear Solutions and for the U.S. Department of Energy under contract number DE-AC09-08SR22470. The Department of Energy's Kansas City National Security Campus is operated and managed by Honeywell Federal Manufacturing Technologies, LLC under contract number DE-NA0002839.

## REFERENCES

- [1]. Ganesh, P., Kaul, R., Paul, C. P., Tiwari, P., Rai, S. K., Prasad, R. C., & Kukreja, L. M. (2010). Fatigue and fracture toughness characteristics of laser rapid manufactured Inconel 625 structures. *Materials Science and Engineering: A*, 527(29), 7490-7497.
- [2]. Edwards, P., & Ramulu, M. (2015). Effect of build direction on the fracture toughness and fatigue crack growth in selective laser melted Ti-6Al-4V. *Fatigue & Fracture of Engineering Materials & Structures*, 38(10), 1228-1236.
- [3]. Seifi, M., Dahar, M., Aman, R., Harrysson, O., Beuth, J., & Lewandowski, J. J. (2015). Evaluation of orientation dependence of fracture toughness and fatigue crack propagation behavior of as-deposited ARCAM EBM Ti-6Al-4V. *Jom*, 67(3), 597-607.

- [4]. Alsalla, H., Hao, L., & Smith, C. (2016). Fracture toughness and tensile strength of 316L stainless steel cellular lattice structures manufactured using the selective laser melting technique. *Materials Science and Engineering: A*, 669, 1-6.
- [5]. Abd-Elghany, K., & Bourell, D. L. (2012). Property evaluation of 304L stainless steel fabricated by selective laser melting. *Rapid Prototyping Journal*, 18(5), 420-428.
- [6]. Wang, Z., Palmer, T. A., & Beese, A. M. (2016). Effect of processing parameters on microstructure and tensile properties of austenitic stainless steel 304L made by directed energy deposition additive manufacturing. *Acta Materialia*, 110, 226-235.
- [7]. Brown, B. (2014). Characterization of 304L stainless steel by means of minimum input energy on the selective laser melting platform.
- [8]. Carroll, B. E., Otis, R. A., Borgonia, J. P., Suh, J. O., Dillon, R. P., Shapiro, A. A., and Beese, A. M. (2016). Functionally graded material of 304L stainless steel and inconel 625 fabricated by directed energy deposition: Characterization and thermodynamic modeling. *Acta Materialia*, 108, 46-54.
- [9]. Scotti, G., Kanninen, P., Matilainen, V. P., Salminen, A., & Kallio, T. (2016). Stainless steel micro fuel cells with enclosed channels by laser additive manufacturing. *Energy*, 106, 475-481.
- [10]. Brown, Ben, "Characterization of 304L stainless steel by means of minimum input energy on the selective laser melting platform" (2014), Masters Thesis, 7322, [http://scholarsmine.mst.edu/masters\\_theses/7322](http://scholarsmine.mst.edu/masters_theses/7322).
- [11]. ASTM Standard E8, 2015, "Standard Test Methods for Tension Testing of Metallic Materials," ASTM International, West Conshohocken, PA, 2015, DOI: 10.1520/E0008-15A, [www.astm.org](http://www.astm.org).
- [12]. C. San Marchi, B.P. Somerday, and S.L. Robinson, "Permeability, solubility and diffusivity of hydrogen isotopes in stainless steels at high gas pressures", *Intern J Hydrogen Energy* 32 (2007) 100-116.
- [13]. ASTM E1820-99 "Standard Test Method for Measurement of Fracture Toughness", ASTM (1999).

Table 1. Composition of Type 304L austenitic stainless steel powder used in this study.

Fe	Cr	Ni	Mn	Si	Co	Mo	C	S	N	P
Bal	18.5	8.69	1.15	0.40	0.035	0.040	0.014	0.0057	0.093	0.0049

Table 2. Average Mechanical and Fracture Toughness Properties

Type 304L Stainless Steels				J <sub>Q</sub> Fracture Toughness Values kJ/m <sup>2</sup>	
Material Condition	YS MPa	UTS, MPa	Elongation %	As-Built	Hydrogen Precharged
AM As-Built	454	626	36.0	799±238	158±28
AM High Toughness	454	626	36.0	989±94	182±7
AM Low Toughness	454	626	36.0	560±58	156±25
Low Strength Forging	415	637	62.9	2190±109	737±42
High Strength Forging	480	675	55.2	1498±492	760±36

Table 3. Fracture Toughness Values and Specimen Location Identifiers

Condition	Location Identifier	As-Built Fracture Toughness Values kJ/m <sup>2</sup>	Hydrogen-Pre-Charged Fracture Toughness Values kJ/m <sup>2</sup>
High-Toughness Specimens	3B1	998	177, 187
	3A3	869	
	3C1	929, 1041	
	3A9	1110	
Low-Toughness Specimens	3B4	478	180 119 158, 131
	3B2		
	3A1	578, 613	
	3A5	575	

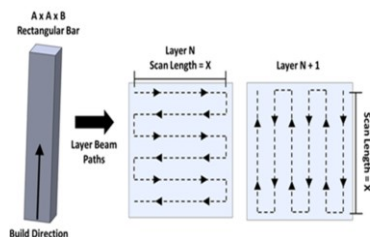


Figure 1. Specimens were built with a common scan strategy (see text).

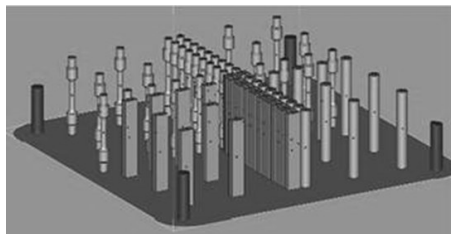


Figure 2. Specimen build geometries used in the Renishaw system showing rectangular 3-pt bend fracture toughness specimens on left.

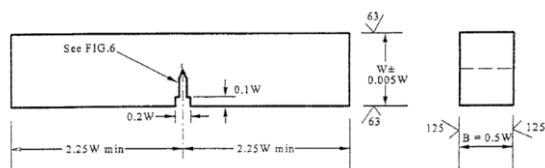


Figure 3. Shape and dimensions of three-point bend fracture-toughness sample. The specimens were 10 mm wide ( $W$ ) and 5 mm thick ( $B$ ) 52 mm long.

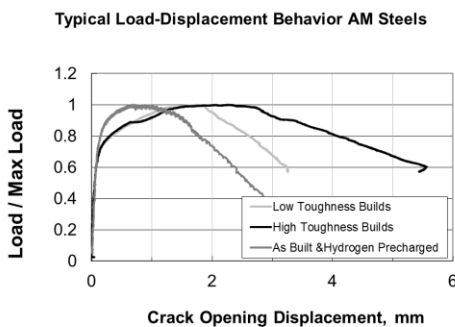


Figure 4. Typical Load-Crack Opening Displacement Behavior for As-Built and Hydrogen Precharged Stainless Steels.



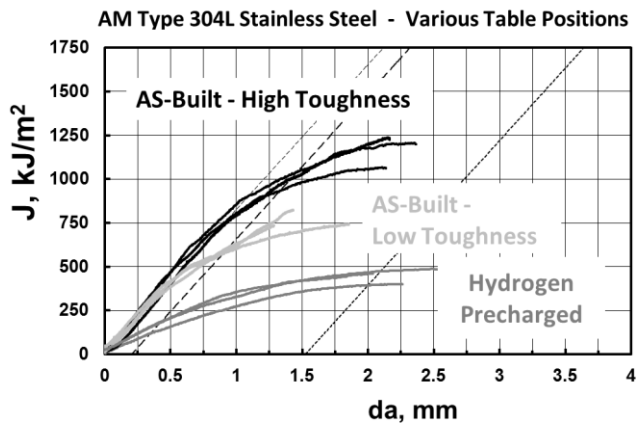


Figure 5. *J-R curves for non-charged and hydrogen precharged specimens.*

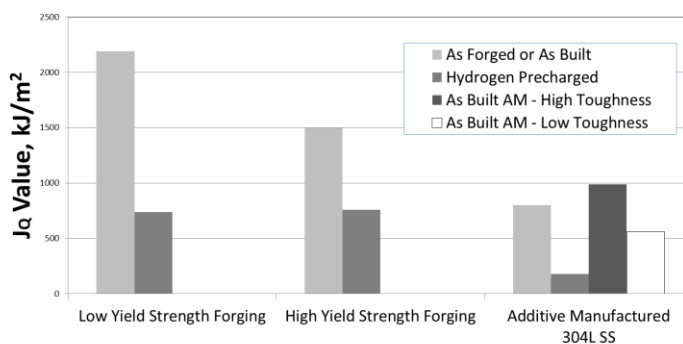


Figure 6. *Comparison of fracture toughness values of AM steels with forged steels.*

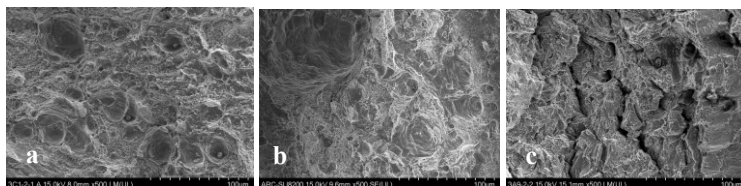


Figure 7. *Fracture appearance of AM steels: (a) As-built high toughness; (b) as-built low toughness; and (c) hydrogen-precharged.*